Risk discrepancies in COVID-19-related community environments based on spatiotemporal monitoring

Jihong Zhang,[1] Guohua Yin,[1] Qiuhua Zhang,[2] Juan Fang,[1] Duo Jiang,[1] Chao Yang,[1] Na Sun[1]

[1]Department of Laboratory Medicine/Clinical Laboratory, Southwest Petroleum University, Chengdu, Sichuan; [2]Department of Dermatology, Heze Traditional Chinese Medicine Hospital, Heze, Shandong, China

Abstract

The geo-inequality of COVID-19 risk has attracted a great deal of research attention. In this study, the spatial correlation between community environment and the incidence of COVID-19 cases in 30 Chinese cities is discussed. The spread of the disease is analyzed based on timing and spatial monitoring at the km^2-grid level, with the use of publicly available data relating to housing prices, Gross Deomestic Product (GDP), medical facilities, consumer sites, public green spaces, and industrial sites. The results indicate substantial geographical variations in the distribution of COVID-19 communities in all 30 cities. Significant global bivariate spatial dependence was observed between the disease and housing prices (Moran's I =0.099, p<0.01, z=488.6), medical facilities (Moran's I = 0.349, p<0.01, z=1675.0), consumer sites (Moran's I =0.369, p<0.01, z=1843.4), green space (Moran's I =0.205, p<0.01, z=1037.8), and industrial sites (Moran's I =0.234, p<0.01, z=1178.6). The risk of COVID-19 under the influence of GDP is further examined for cities with per capita GDPs from high to low ranging from 1.69 to 4.62 (1.69~3.74~4.62, 95% CI). These findings provide greater detail on the interplay between the infectious disease and community environments.

Correspondence: Na Sun, Department of Laboratory Medicine/ Clinical Laboratory, Southwest Petroleum University, Chengdu, Sichuan, China.
Tel.: +8613258003887 - Fax: 02889364148
E-mail: 527226058@qq.com

Key words: COVID-19 risk, community environments, economic inequality, China.

Conflict of interest: the authors declare no potential conflict of interest, and all authors confirm accuracy.

Availability of data and materials: all data generated or analyzed during this study are included in this published article.

Funding: this research received found from the following institutions: the Fundamental Research Funds for the Central Universities under Grant KYTZ202278; the Natural Science Foundation of Sichuan Province under Grant 2023NSFSC0751; the Science Popularization Education Project of Hepatitis elimination by 2030 under GrantXCGY202401; the Higher Education Science Research Planning Project under Grant24BJ0420.

Acknowledgments: we would like to extend our sincere gratitude to Associate Professor Sang Xuejia from Chengdu University of Information Technology for his significant contributions to the proposal of the research idea and the conduct of the experiments in this study. We thank the professor Jing Yang and doctor Xing Ge of Xu Zhou Medical University for their assistance Guiding the application of public health-related knowledge, and correcting language error of an early version of this manuscript.

Received: 23 March 2024.
Accepted: 28 February 2025.

Geospatial Health 2025; 20:1286
doi:10.4081/gh.2025.1286

Introduction

Ensuring equal health rights with regard to COVID-19 during the pandemic for middle- and low-socioeconomic residents has been a significant challenge Since the infection has resulted in an unusually high number of infections and deaths globally and led to a global economic recession and medical runs. According to the Demographic and Health Surveys (DHS) Program, this has impacted the health rights of low-socioeconomic groups negatively (DHS, 2020; Hopkins, 2020). Examples include the abilities of less developed countries to provide sufficient Polymerase Chain Reaction (PCR) testing, medical treatment and social security (Ahmad *et al.*, 2020; Finch & Hernández Finch, 2020). The inequalities of COVID-19, including economic, environmental and medical inequalities that have resulted from it, have become serious, social issues (Buikema *et al.*, 2021; Price-Haywood *et al.*, 2020; Woo & Jun, 2021).

High-resolution COVID risk analysis is of particular importance for pandemic prevention and control (Sousa *et al.*, 2022; Yang *et al.*, 2021). However, when examined on the community scale, its various influences on the urban environment become intricate and difficult to disentangle (Cordes, 2020; Yang *et al.*, 2021). Many factors can affect the health of residents, including the amount of fast-food restaurants, hospitals, green spaces and factories in a neighbourhood, and it has been shown that geographical factors contribute to several chronic diseases, such as high blood pressure, obesity and asthma (Lantz *et al.*, 1998; Pearson, 2015). In addition, neighbourhood characteristics may result in higher infection rates and poorer health outcomes among disadvantaged populations, paricularly in poorer areas, due to a lack of public trust in government and health authorities (Pak *et al.*, 2020) and limited access to healthcare (Dowd *et al.*, 2020; Pettinicchio *et al.*, 2021). During previous epidemics and pandemics, researchers have reported that the targeting of commuters from high-incidence locations (Cuong *et al.*, 2013) and low socioeconomic areas (Barmby & Larguem, 2009; Hansen *et al.*, 2016; Skatun, 2003) can help mitigate the transmission of the disease in these communities. On this basis, some researchers believe that the community environment is a potential reason for the inequity of COVID (Jim & Chen, 2006). Due to the correlation of social statistics with environmental indicators, multi-source, spatial big data were obtained using a big 'data sniffer' for this experiment enabling the construction of six basic data layers, including community infrastructure, public green space, consumer sites, medical sites, industrial sites and economic environment (Qian *et al.*, 2021; Zheleznyak & Khripach, 2014). This experiment analyzes the spatial correlation between multiple indicators of the urban environment in addition to that between COVID risk and the urban environment. Together with the community-level COVID-19 data that was authorized and released by the Chinese center of Disease Control (CDC), a block-scale, COVID-19 dataset was constructed. This dataset was then used to verify the relevant assumptions relating to whether or not poor community environments face a higher COVID-19 risk than others.

Materials and Methods

COVID-19 data

The COVID-19 data used in this study was obtained from Alibaba and authorized by the Chinese CDC (Platform, 2020). The COVID-19 data used in this study are from publicly available sources and available at the website: https://pages.uc.cn/r/feiyan-map/FyMapPageMap. A community pandemic data monitoring system was established for observing the community data of confirmed COVID-19 cases announced by the health departments of prefecture-level cities. The main functional modules of the sniffing system were based on the 'Beautiful Soup' library (Pant *et al.*, 2024) and the three core modules: the sniffing module, the parsing module and the storage module. Several main functions including parameter construction, timing, polling and exception handling were included. The geographic analysis function was built around Baidu Map Geocoding's Application Programming Interface (API), with the quality of the geographic analysis controlled by manual inspection. The core part of the system source code was uploaded as an attachment. For this study, all communities identified as COVID-infected were those with at least one confirmed case. According to the description of the data source from the Chinese CDC, a confirmed case is defined as a laboratory-confirmed case or a case that meets the clinical case definition and is epidemiologically linked to a confirmed case.

Data on the communities where confirmed COVID-19 patients were found was obtained and Figure 1 was plotted as a means of comparing multiple COVID-19 outbreaks in mainland China in terms of time and total infections. From 2019 to 2021, the most significant period of the COVID-19 pandemic, occurred between January and March 2020. In this period, large number of people were infected and it lasted a long time exhibiting a clear complete three stages consisting of a beginning, a middle and an end. We therefore chose this period (January 2020 to March 2020). China CDC defined a confirmed a COVID-19 patient as either a laboratory-confirmed patient or a case that satisfies the clinical case definition including an epidemiologic link to a confirmed patient. In this study, each community was treated as a research individual, and a case was defined as a community with confirmed COVID-19 patients. Regardless of the number of COVID-19 patients found in a community, it was marked "with COVID" in order to reduce the impact of demographic factors in the absence of community-resolution population data. Due to an insufficient number of affected communities in several cities, this experiment excluded 163 cities (average 7.5 communities/city) and focused on 2,387 communities in 30 cities (average 79.6 communities/city). Each piece of data in the early stage of the pandemic was regarded as extremely valuable and such data are of great significance for understanding the prevention and control measures as well as the transmission pathways. During the data processing in this study, only the cities with overly low case counts were removed, and no excessive manual interventions were made.Key tracking analysis was then conducted for these 30 cities and community cases data continued to be obtained.

Monitoring

Spatial monitoring of COVID-19 was monitored basedon the community environment. Housing prices were used as a direct benchmark for the community infrastructure as they reflect the ambient socioeconomic level. These data were obtained from one of the largest real estate online transaction platforms in China, 58.com (Inc). Field interpolation is a mature method for supplementing missing data in the fields of real estate and geographic information (van den Broek-Altenburg *et al.*, 2020; Cellmer, 2011; Crosby *et al.*, 2018). The average housing price data for a total of 50,796 communities in 30 cities was interpolated and used as the basic data for community infrastructure.

We obtained data on Points Of Interest (POIs) and land use from Openstreet.com, which is the largest open-source map data source in the world, including Medical facilities (M), Consumer sites (C), public Green spaces (G) and Industrial sites (I) referred to as MCGI When presented together. This data was interpolated with Euclidean distances into a continuous grid matrix that represented the shortest distance from any point to the nearest MCGI within the 30 city precincts. A total of six consecutive spatial matrices with 1-km resolution, including the distance to COVID community (D2COVID); to medical site (D2Med); to public green space (D2Green); to consumption place (D2Consum); to industrial site (D2Ind); and the interpolated house price (HP), were used for analyzing the environmental impact of community COVID risk.

The bivariate spatial autocorrelation between 1-km^{2}grid-level environmental factors and the location of confirmed COVID-19 cases was measured using Moran's Index, the most common global spatial autocorrelation measurement, which gives the overall distribution of departures from randomness. Univariate and bivariate global and the Local Indicators of Spatial Association (LISA) were used at the grid level for providing information on various forms of spatial correleations, such as autocorrealtion, clusters and outliers. The LISA calculation was based on Queen's contiguity spatial-lag of order 1, and the statistical significance of the spatial autocorrelation pattern in each grid (relative to the entire spatial scope) was tested at a 5% level of significance (p=0.05). The spatial dependence of the grid was plotted on the map and colour-coded based on the type of interaction.

Bivariate global spatial autocorrelation results reveal the spatial correlation between two variables and its significance indicates whether a positive or negative spatial correlation is obvious. Aggregation types can be divided into four types: high-high (HH), LL (low-low), high-low (HL), and low-high (LH). It is important to note that the COVID-19 and MCGI parameters used in this experiment were distances, so the corresponding four types of aggregation have different meanings. HH aggregation suggests a low impact of COVID-19 risk and environmental factors, while LL type aggregation means that is the impact is high. HL clusters indicate a lower risk of COVID-19 but a higher impact of environmental factors, while LH clusters indicate a higher risk of COVID-19 with a lower impact of environmental factors. HH and LL clusters indicate a positive correlation between COVID-19 and the impact of environmental factors, whereas HL and LH clusters show a negative correlation between COVID-19 risk and the impact of environmental factors. By using these approaches, it was hoped to spatially monitor community environmental indicators for anomalies relating to COVID-19 risk.

The time-series variation characteristics of global and local spatial autocorrelation of the COVID-19 epidemic in 30 cities analyzed from community scales using global and local Moran's *I*, cluster, and outlier analysis reulted in basic data from 53,183 communities in 30 cities. The house price and MCGI data were then formatted into a 1-km grid, with a total of 414,173 for subsequent correlation and Moran's analysis. In addition, five time-sections of COVID data from between February and March were combed for analyzing the shift of the pandemic in 30 cities across the community infrastructure level.

Temporal monitoring of COVID-19 basedon housing prices

To follow the evolution of COVID risk in the 30 cities, we simplified the monitoring of the mobile component of the COVID risk by dichotomization of the communities into those with a highlevel of infrastructure and those in the opposite situation based on the average housing price of the city in question. The processing of the average house price was performed in two steps;firstly, the house price information for every community in each city was obtained using a network sniffer,then ArcGIS (ESRI, Redlands, CA, USA) was used to count the average price of all communities within the jurisdiction of each city to determine the average house price.

The number of communities with COVID-19 patients and the number of communities without in the two community infrastructure categories were counted, and a contingency table for each city was established (Table 1). We calculated the COVID-19 patients for each community just once to reduce the impact of differences in the population of communities. The communities located in the low infrastructure level area were labelled exposure variables, and if COVID-19 was found they werelabelled outcome variables. This enabled the calculation of the COVID-19 odds ratio for the low community infrastructure level. As there were different development levels between cities, this study introduced per capita GDP and further conducted Spearman rank correlation analysis between different cities as a means of verifying the statistical regression relationship between the economic level and the COVID-19 odds ratio.

We used used big data timing snapshots for monitoring community-level time series COVID data in China. The COVID data for each time section was counted by community infrastructure coordinates and plotted as a time-series using the nonparametric testing method Kernel Density Estimation (KDE). Assuming ($x1, x2, \dots, xn$) to be a univariate independent sample with similar distribution characteristics drawn from the f distribution with unknown density, the shape of the estimated function f is of great interest. The distribution of the KDE curve f can be defined as:

$$f_h(x) = \frac{1}{n}\sum_{i=1}^{n} K_h(x - x_i) = \frac{1}{nh}\sum_{i=1}^{n} K\left(\frac{x - x_i}{h}\right) \qquad \text{(Eq.1)}$$

where K is the kernel (a non-negative function) and $h > 0$ is a bandwidth smoothing parameter. The K_h is the zoom kernel and is defined as $K_h(x) = 1/hK(x/h)$. This affects the microscopic fitting accuracy of curve f, but has no effect on the macroscopic distribution law of the curve. Generally, a series of kernel functions is used for the K kernel, including the uniform function, triangle function, double weight function, triple weight function, Epanechnikov function and the normal distribution function. The standard normal distribution function kernel is generally used for reducing the calculation scale, meaning that $K(x) = \varphi(x)$, where φ is the standard normal density function (Figure 2 and S1 video).

Infectious diseases are spread from the source of infection to all people who are susceptible. From the time cross-section of price data, it was found that communities where COVID-19 cases

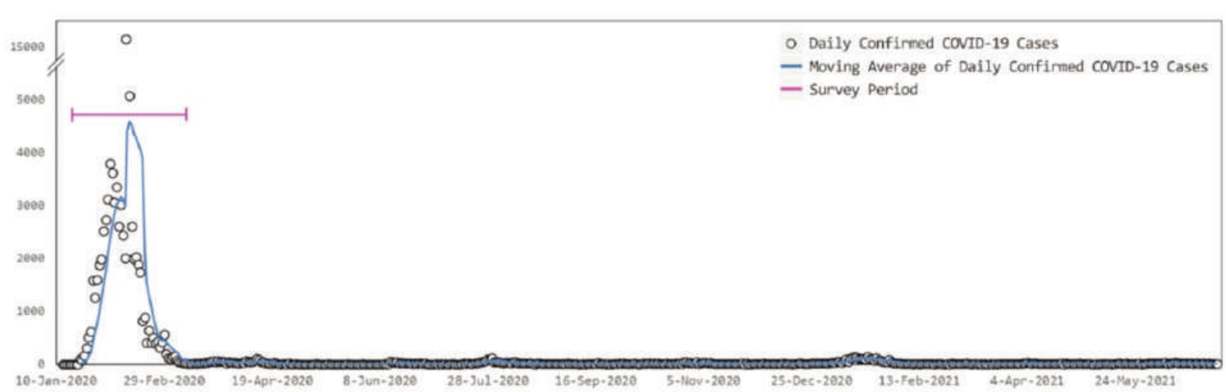

Figure 1. The duration of the data survey and China's epidemic situation. Theabscissa (the horizontal X-coordinate) represents the time line and the ordinate (the vertical Y coordinate) represents the number of people diagnosed with COVID Chinese mainland. This experiment selected the largest outbreak of COVID-infected people in China, January to March 2020.

appear are not confined to the original price range, so an increase in the number of other price ranges can occur. This will result in the price distribution KDE curve shifting along the X-axis, so its mean and variance will also change. From the change in the normal distribution μ of the price-distribution curve of the diseased cell, it can be seen that there a two states to the relative position change based on the time sequence: μ1 > μ2 and μ1 < μ2. By combining the distribution of the initial curve, it can be judged whether the distribution curve is approaching or deviating from the background (BG) distribution, which can be used as an indicator teling whether the COVID-19 pandemic at the community scale of a region is in a state of local or regional spreading.

In order to quantify the extent to which the curve moves to the background value based on the linear regression function of the housing price and frequency distribution $X \sim N(\mu,\sigma^2)$ of the diseased community, we propose Community Infection Trends (CIT) a quantitative measure to be used for quantifying the tendency of housing prices in communities with COVID patients when deviating from the ideal distribution axis of symmetry:

$$CIT = \left| \frac{\sum(\sigma_{is} - \bar{\sigma}_s)(y_i - \bar{y})}{\sum(\sigma_{is} - \bar{\sigma}_s)^2} \right| \qquad \text{(Eq.2)}$$

$$\sigma_{is} = \left(\frac{\sigma_i - \bar{\sigma}}{\bar{\sigma}}\right)\left(\frac{\sum y_i}{\sum \sigma_i}\right) \qquad \text{(Eq.3)}$$

In Eq. 3, σ_{is} is the normalized price curve movement and $\left(\frac{\sigma_i - \bar{\sigma}}{\bar{\sigma}}\right)$ used for offsetting the absolute difference in housing prices in different cities.

In Eq. 4, $\left(\frac{\sum y_i}{\sum \sigma_i}\right)$ was used for balancing and standardizing the sample data, with*y*as the time index. The index is able to quantify the law of temporal spread, determine whether the city is in a state of local spread (negative value) or regional spread (positive value) and indicates also the severity of its quantitative changes.

Table 1. Baseline information of of home prices in relation to COVID-19 risk in 30 cities.

City	Local price (mean)	Local price (SD)	CwC price (mean)	CwC price (SD)	CwC price (<mean)	CwC price (>mean)	CnoC price (<mean)	CnoC price (>mean)	Pearson chi-square	P	AUC
Anqing	7,654	2,000	6,472	1,249	31	11	581	601	9.52	2.0E-3	0.70
Bengbu	6,751	2,190	6,797	1,541	56	34	332	354	5.38	2.0E-2	0.48
Bozhou	6,157	1,774	7,848	3,806	23	25	211	209	0.08	7.7E-1	0.59
Changde	6,097	1,841	6,561	3,147	31	28	500	504	0.16	6.9E-1	0.76
Changsha	9,883	4,221	9,749	2,556	84	52	1,955	1,988	7.55	6.0E-3	0.47
Chengdu	17,710	7,731	21,257	6,803	5	8	280	277	0.69	4.1E-1	0.31
Chongqing	9,550	4,915	7,054	5,174	65	12	476	529	36.48	1.5E-9	0.70
Fuyang	7,445	2,271	6,782	1,620	69	41	385	413	7.13	7.6E-3	0.58
Guangzhou	28,399	16,584	28,213	14,026	122	77	4,443	4,488	10.18	1.4E-3	0.48
Harbin	9,171	4,836	8,658	3,054	63	64	1550	1,550	0.01	9.3E-1	0.48
Hefei	14,985	4,710	13,948	4,555	57	30	847	874	8.38	3.8E-3	0.62
Huaihua	5,023	1,304	4,413	788	22	7	263	278	7.76	5.4E-3	0.67
Jiujiang	6,582	2,511	9,210	3,300	18	41	611	588	8.97	2.8E-3	0.61
Liu'an	6,935	1,550	5,396	757	34	4	220	250	23.68	1.1E-6	0.80
Nanchang	12063	4,316	10,897	3,419	90	35	1,312	1,367	24.2	8.7E-7	0.60
Nanyang	7,049	2,834	5,297	1,791	61	14	616	664	29.52	5.5E-8	0.68
Neijiang	5,609	1,581	6,234	3,565	22	10	371	383	4.5	3.4E-2	0.64
Ningbo	18,598	8,528	20,939	9,236	28	54	1,988	1,962	8.24	4.1E-3	0.51
Pingdingshan	6,382	1,680	5,630	690	26	7	143	162	10.94	9.4E-4	0.64
Quanzhou	9,461	4,686	6,848	1,138	53	1	1213	1265	50.07	1.5E-12	0.64
Shangqiu	4,675	1,588	3,893	760	61	12	635	684	32.89	9.8E-9	0.68
Shangrao	6,845	1,689	6,127	2,075	54	16	553	591	20.63	5.6E-6	0.73
Shenzhen	5,0670	33,984	55,764	23,104	86	104	1,792	1,774	1.71	1.9E-1	0.46
Suzhou	34,969	17,166	41,493	1,6488	5	10	236	231	1.67	2.0E-1	0.37
Xinyang	5,686	2,044	4,887	1,052	134	29	519	625	67.8	1.8E-16	0.63
Xinyu	5,528	1,500	4,547	757	74	12	130	192	44.7	2.3E-11	0.72
Yiyang	4,775	1,562	5,078	1,940	24	11	278	291	4.83	2.8E-2	0.72
Yueyang	6,268	2,049	5,332	1,539	60	24	434	470	15.43	8.6E-5	0.66
Zhengzhou	14,304	6,299	13,083	5,328	18	8	491	501	3.85	5.0E-2	0.58
Zhuzhou	5,601	1,468	4,927	904	51	16	500	536	18.35	1.8E-5	0.65

CwC, community with COVID; CnoC, community without COVID; AUC, area under the curve.

Controlled experiments for other social statistical factors

A city-scale controlled experiment was also designed and the relationship between the indicators (population, age structure, family size, years of education, illiteracy rate, housing price, GDP) and the proportion of communities with COVID-19 patients at the city scale was analyzed. In an attempt to evaluate the impact of common indicators mentioned in other studies on the risk of the probability of finding COVID-19 cases in a community (PFCC), they were compared to the impact of housing price factors before analyzing the housing price indicators at the community resolution and the urban-specific data for population was retrieved from the Sixth National Population Census of China. This included total population, those aged 0-14, 15-59, and >60 years, family size, years of education, and literacy rate. Therefore, this demographic data was correlated with the PFCC at the urban resolution, and the relationship between house prices, per capita GDP, and the proportion of communities with COVID-19 patients were analyzed simultaneously to compare population, age structure, education and economic factors and the degree of correlation with COVID-19 on the city scale. The urban-scale housing prices were obtained from the average community-level house prices in the urban area, and the GDP data was obtained from the 2019 China Statistical Yearbook.

Experimental environment and parameters

A big data crawler was drawn with Python (v.3.7). The source code was released under the GNU v3 license and was accessible at https://github.com/qq5220243/COVID _HousingPrice. In order to evaluate possible correlations and the interplay between different parameters, separate analyses were run considering one of the parameters as the independent variable, with the measures odds ratio, Area Under the Curve (AUC), GDP and housing price as dependent variables, and other parameters for defining particular experimental settings (see Results for details). Geoda 1.14 was used for performing geographic analysis relating to Moran's *I*results. Other analyses were performed using R version 3.5.3. Kriging interpolation, data extraction, correlation analysis, and clustering analysis. These analyses were performed using the Spatial Analyst Tools of AcGIS 10.5; Geocoding performed with Baidu Map JavaScript API v2.0 and ArcGIS; and the maps in the manuscript drawn using ArcGIS and QGIS.

Results

Basic information

Table 2 displays the statistical characteristics of the urban resolution of 30 cities, and 11 base indicator data were counted. The average GDP of the 30 cities was found to be 84.49 with a Standard Deviation (SD) of 86.24, and the average population was 616.99 (SD: 364.35). The average housing price was 11,360.79 (SD: 10,032.65), with a high variance between house prices in dif-

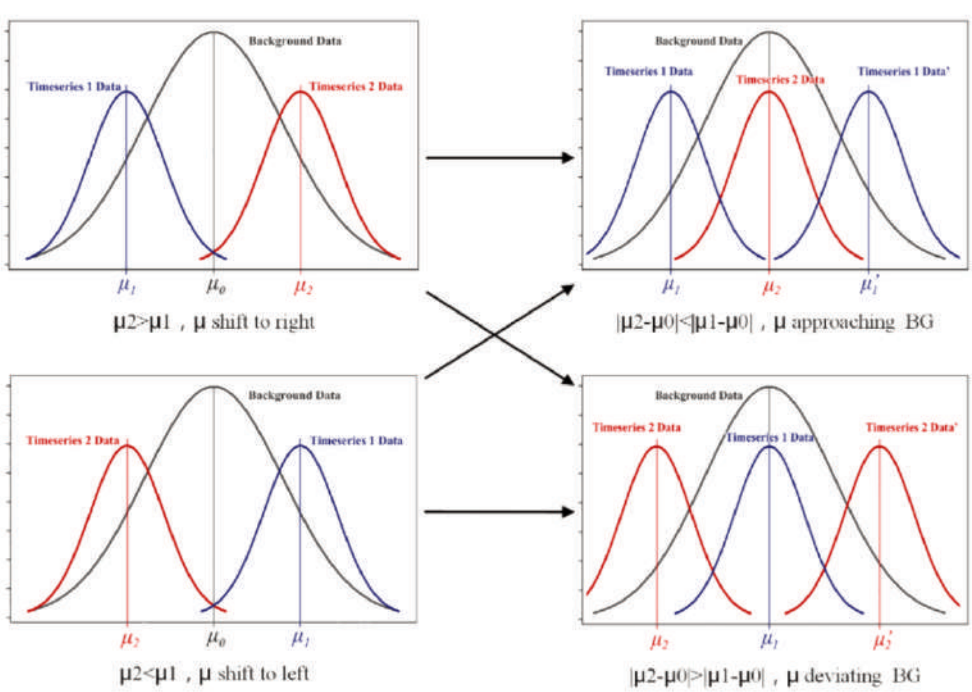

Figure 2. The house price frequency time series of the spread of COVID-19. The X coordinate of each subgraph is the housing price of the community, and the Y coordinate represents the frequency. The black curve in the subgraph represents the background distribution (BG) of housing prices for all neighbourhoods of the city. The coloured curve represents the distribution of housing prices in communities where people with COVID are found. Among them, blue represents the distribution of house prices at time 1, and red represents time 2. With the different patterns of the spread of the epidemic, communities with different house prices are infected with COVID, and the house price curve will shift on the abscissa, which can be represented by the μ of the curve.

pagepress

ferent cities. House prices also showed high variability within each city, with Coefficients of Variation (CVs) ranging from 0.22 to 0.58, and an average of 0.37 (SD: 0.11). There were 2,324 community data counts (as of March 14th, 2020) where COVID-19 was discovered in 30 cities, with an average closest distance of 3,050m (SD: 5464m).

COVID-19 risk at city scale

As Figure 3 shows, base statistical analysis displays a statistical relationship between population (p=0.41, n=30), population of people aged > 60 years (p=0.10,n=30), but the PFCC, and this relationship was not found to show statistical significance. A weak linear correlation between family size and PFCC (r=0.38, 95% CI, n=30) was discovered in a Spearman rank correlation test. Other indicators, population of 0-14 years (r=0.43, 95% CI, n=30) and literacy rate (r=0.496, 95% CI, n=28) exhibited a moderate linear correlation with PFCC. However, astatistically significant strong linear correlation was found between years of education and the PFCC (r=-0.53, 95% CI, n=30). Strong statistically significant correlations were also found between per capita GDP and PFCC (r=-0.56, 95% CI, n=30), house price and PFCC (r=-0.598, 95% CI, n=30) and the 15–59 years old population section and PFCC (r=-0.65, 95% CI, n=30). These data supportthe housing price as a strongly associated factor, at least in urban areas. This represents the market recognition of the community infrastructure, which is often expressed in price, and its correlation with the COVID risk

Table 2. The statistical characteristics of the urban resolution of 30 cities.

City	Number of people in the different age groups x 10^4					Average number of persons per household	Illiteracy rate (%)	Education (>15 years)	Proportion CwC	Average house price (RMB/m^2)	GDP per capita (RMB x 10^3)
	0-14 (years)	15-59 (years)	60-65 (years)	65+ (years)	60+ (years)						
Anqing	16.68	61.81	4.44	17.06	21.5	2.57	2.71	9.18	0.03	7,654	36.3
Bengbu	22.21	59.8	3.63	14.4	18.03	2.74	5.31	9.19	0.12	6,751	40.7
Bozhou	25.6	57.9	2.9	13.61	16.51	2.72	6.95	8.38	0.10	6,157	24.4
Changde	14.87	60.1	0.86	19.16	20.02	2.6	1.6	9.5	0.05	6,097	58.2
Changsha	16.64	68.03	4.22	11.11	15.33	2.62	0.47	11.52	0.03	9,883	134.9
Chengdu	13.28	68.74	4.36	13.62	17.98	2.49	1.7	10.85	0.02	17,710	117.2
Chongqing	15.91	62.22	4.79	17.08	21.87	2.45	1.63	9.8	0.09	9,550	79.8
Fuyang	24.44	58.69	3.09	13.79	16.88	2.85	5.72	8.51	0.12	7,445	16.4
Guangzhou	13.87	74.72	3.59	7.82	11.41	2.22	0.58	11.61	0.02	28,399	158.5
Harbin	10.46	67.56	7.33	14.65	21.98	2.23	2.67	9.93	0.05	9,171	55.2
Hefei	16.5	68.2	3.3	12	15.3	2.52	3.72	10.08	0.05	14,985	116.4
Huaihua	20.24	58.68	5.2	15.88	21.08	2.6	2.69	9.16	0.05	5,023	30.4
Jiujiang	20.96	61.37	4.95	12.62	17.57	2.74	2.51	9.74	0.05	6,582	55.1
Liu'an	18.53	60.21	4.4	16.86	21.26	2.53	2.83	8.98	0.07	6,935	20.7
Nanchang	17.44	67.59	4.43	10.54	14.97	2.81	1.93	11.01	0.05	12,063	95.1
Nanyang	26.23	54.99	4.57	14.22	18.79	2.86	2.09	9.14	0.06	7,049	35.6
Neijiang	15.55	59.22	5.2	20.03	25.23	2.39	3.84	8.72	0.04	5,609	34.3
Ningbo	12.26	69.63	5.51	12.59	18.1	2.21	1.55	9.97	0.02	18,598	131
Pingdingshan	24.78	56.92	4.77	13.53	18.3	2.98	2.02	9.63	0.10	6,382	41
Quanzhou	20.62	66.17	4.21	9	13.21	2.74	1.94	9.3	0.02	9,461	114.3
Shangqiu	25.42	56.44	4.12	14.02	18.14	2.64	3.4	9.88	0.05	4,675	32.6
Shangrao	23.23	59.08	5.24	12.45	17.69	3.11	2.45	9.27	0.05	6,845	26.3
Shenzhen	15.11	79.53	2.03	3.33	5.36	2.25	1	11.86	0.05	50,670	206.7
Suzhou	13.55	69.49	4.52	12.44	16.96	2.62	2	10.67	0.03	34,969	475.5
Xinyang	23.67	57.06	4.07	15.2	19.27	2.66	4.06	8.89	0.13	5,686	27
Xinyu	20.73	61.59	5.43	12.25	17.68	2.76	2.72	9.85	0.22	5,528	93.9
Yiyang	17.71	59.65	5.47	17.18	22.65	2.54	1.73	9.31	0.06	4,775	40
Yueyang	18.46	61.27	5.27	15	20.27	2.76	1.27	10.06	0.09	6,268	60
Zhengzhou	19.05	68.11	3.86	8.98	12.84	2.82	0.88	11.76	0.03	14,304	111.7
Zhuzhou	18.28	61.8	5.39	14.53	19.92	2.78	0.91	10.21	0.06	5,601	65.4
Mean	18.74	63.22	4.372	13.50	17.87	2.63	2.57	9.87	0.06	1,136	84.49
SD	4.25	5.71	1.176	3.36	3.80	0.22	1.51	0.94	0.04	1,003	86.21
CV	0.23	0.09	0.269	0.25	0.21	0.08	0.59	0.10	0.66	0.88	1.02

CwC, community with COVID; RMB, Chinese yuan, the official currency of the People's Republic of China; GDP, gross domestic. product.

(Figure 3). The analysis of 414,173 data grids found an incredibly significant correlation between the six types of data ($p<0.01$, Figure 4). The correlation coefficients between D2Consumer and D2Greenspace as well as D2Consumer and D2Medical reached 0.702 and 0.666, respectively, which indicate a significant positive correlation for these two data pairs. The correlation coefficients of D2COVID and the four components of MCGI also reached 0.352, 0.373, 0.208 and 0.235, respectively, indicating they allhave a tendency to appeart together as a concentrated reflection of COVID-19 risk. A statistically significant negative correlation between the distribution of house prices and MCGI (-0.276, -0.262, -0.279, -0.167), which is consistent with the idea that community medical care, green spaces, consumption and industrial sites result in high housing prices. However, an incredibly strong positive correlation was found between house prices and COVID (0.099), indicating that closeness to a COVID-19 community results in lower house prices. This is the opposite of the COVID-related trend with MCGI, which is of great importance. As Figure 5 show, moderate and high significant global spatial autocorrelation in the distribution of communitywith COVID-19 (Global univariate Moran's I =0.994, $p<0.01$), medical sites (Moran's I =0.994, $p<0.01$),consumer sites (Moran's I =0.991, $p<0.01$), green space (Global uni-

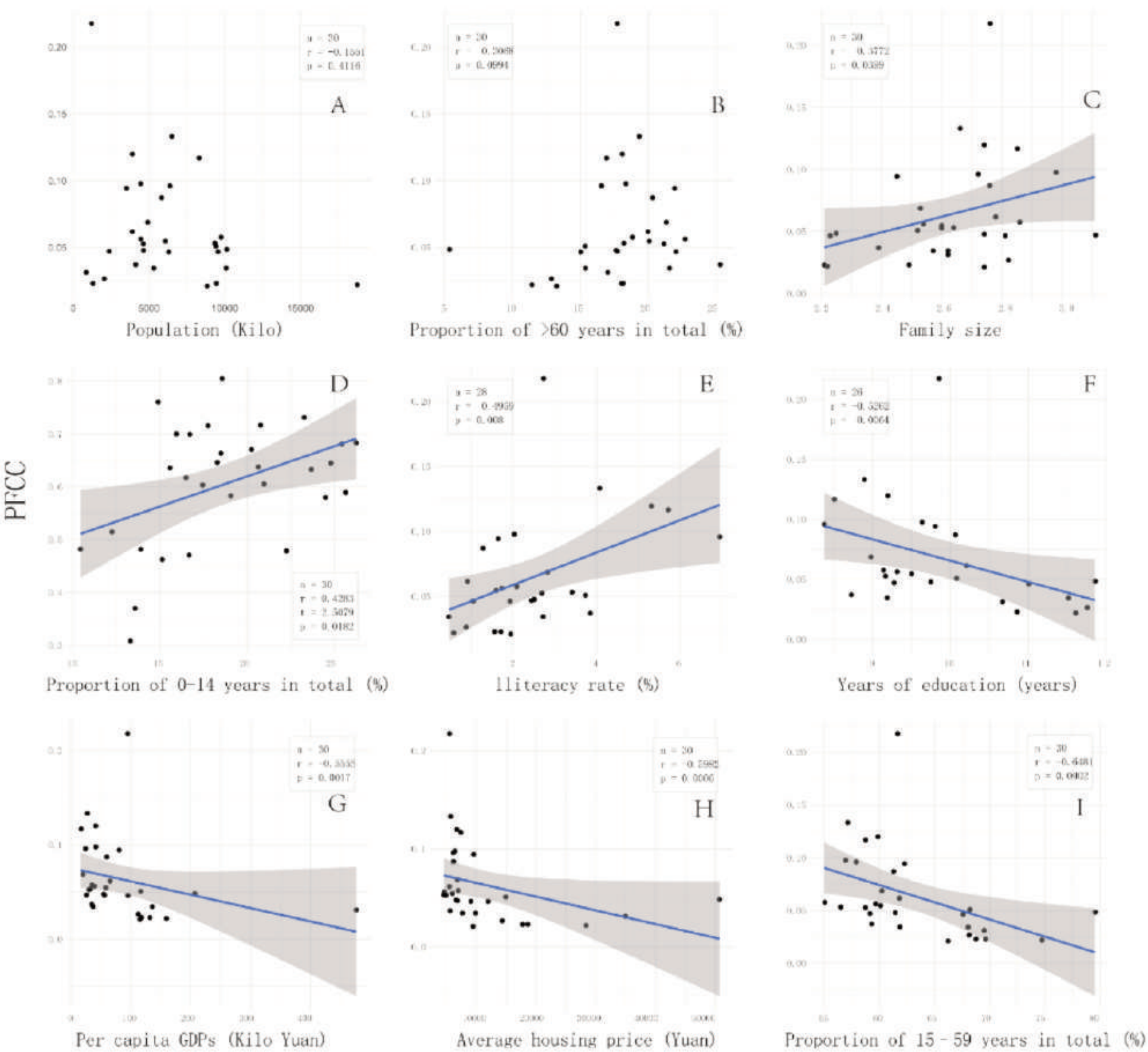

Figure 3. The relationship between the indicators and PFCC at the city scale. The ordinate indicates PFCC (the probability of finding COVID-19 cases in a community), and the abscissa indicates 9 different indicators, including: **A**) population, **B**) proportion of people over 60 years old, **C**) family size, **D**) proportion of population under 14 years old, **E**) illiteracy rate, **F**) years of education, **G**) GDP per capita, **H**) average house price, **I**) proportion of population aged 15-59.

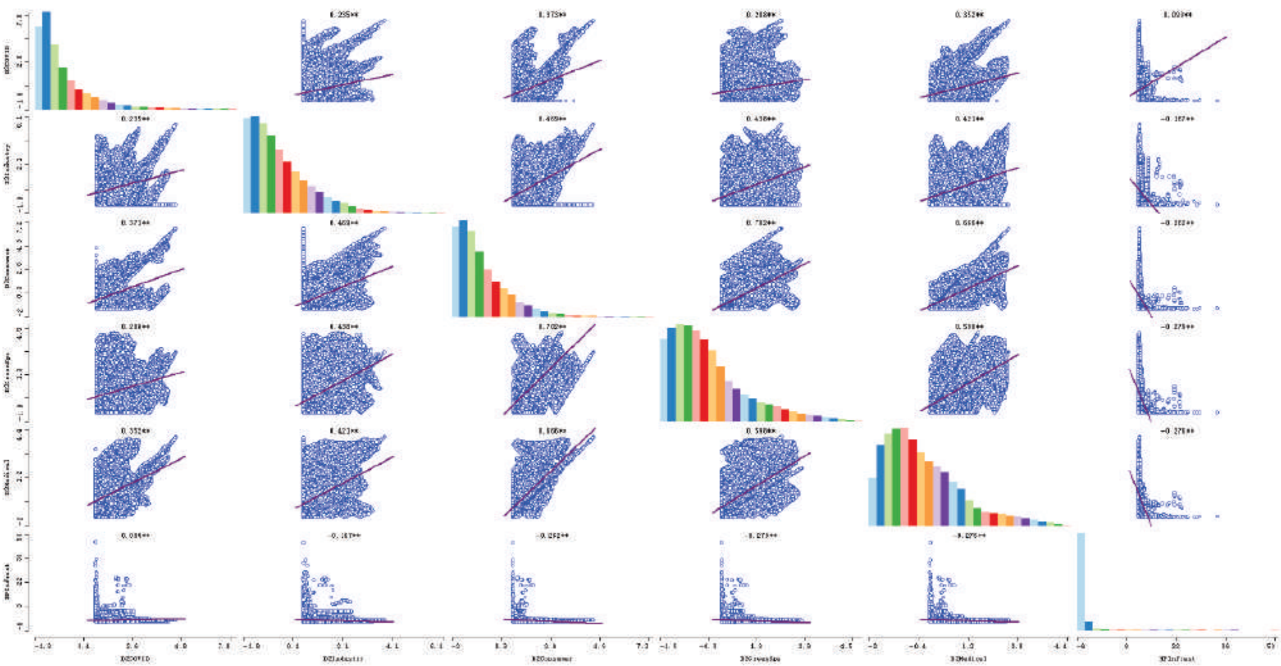

Figure 4. Linear correlation scatterplot matrix of 6 layers. The correlation matrix shows the correlation and linear fit of COVID, industry, consumer, green space, medical sites, and housing prices.

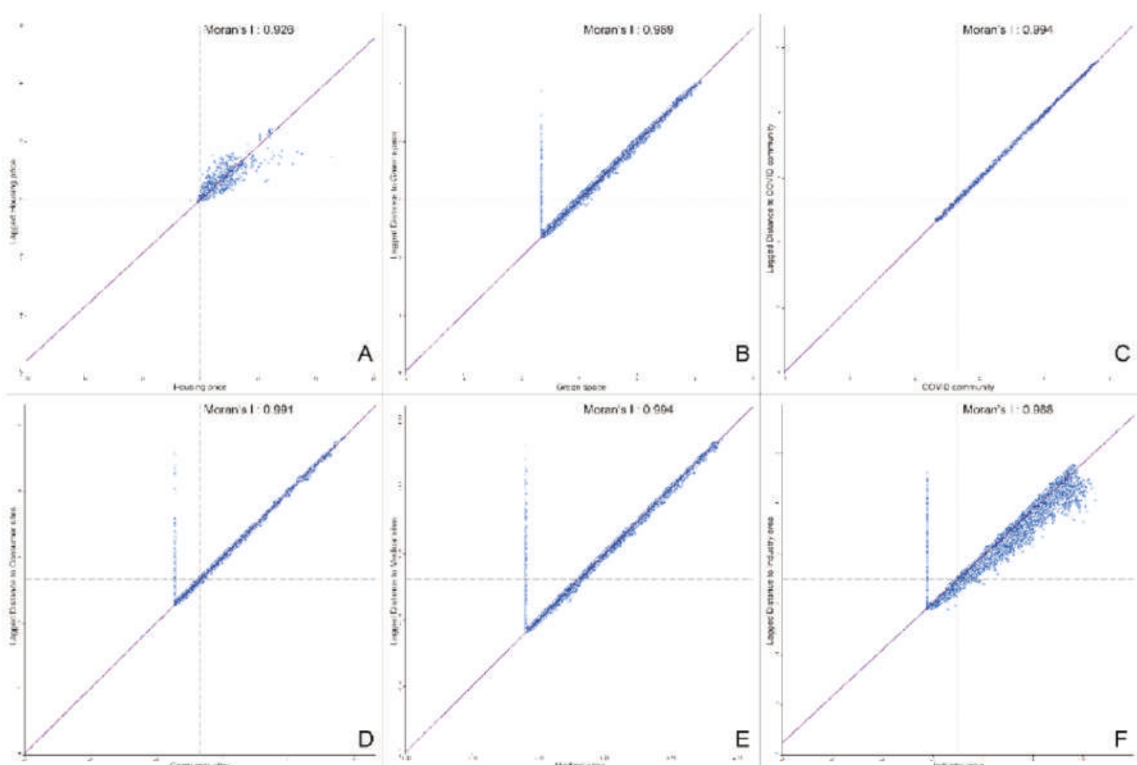

Figure 5. Global univariate Moran's *I* autocorrelation scatterplot of 6 layers. All subplots are normalized. A very high Moran's *I* (>0.9) indicates that these layers exhibit very high spatial autocorrelation. **A**) housing price, **B**) green space, **C**) Covid, **D**) consumer sites, **E**) medical sites, **F**) industry area.

variate Moran's I =0.969, p<0.01), industry area (Moran's I =0.988, p<0.01), and house price (Moran's I =0.926, p<0.01) were observed in the 1-km the grids of the 30 cities. That these Moran's Ivalues werehigher than 0.9 might be related to the collectivist urban planning in China.Certainly, the use of the 1-km grids instead of the commonly adopted administrative divisions can also lead to higher Moran's I values, which is determined by the First Law of Geography (Tobler, 1970).Univariate LISA plots revealed the presence of significant spatial clusters or outliers by grids.

In addition, significant global bivariate spatial dependence (Figure 6) was found between the disease and house price (Moran's I =0.099, p<0.01, z=488.6), medical sites (Moran's I = 0.349, p<0.01, z=1675.0), consumer sites (Moran's I =0.369, p< 0.01, z=1843.4), green space (Moran's I=0.205, p<0.01, z=1037.8), and industrial area (Moran's I=0.234, p<0.01, z=1178.6).When the sample size tends towards infinity, Moran's I tends towards 0. Therefore, for larger sample sizes, even a small Moran's I value (0.099) is acceptable.

As Figure 7 shows, the bivariate Moran's I of medical sites versus COVID maps buffers at lower resolution due to there being fewer medical facilities, but dark blue anomalies in western and eastern cities suggests high risk of COVID with adequate medical coverage, and the dark red color in the Midwest and Northeast shows a low risk of COVID with insufficient medical resource coverage. Large areas of light blue in Central cities show that there is a high risk of COVID in situations with insufficient medical resources. Light red indicates a low risk of COVID in a community with a good healthcare environment. These areas are mostly concentrated in satellite cities around the provincial capitals, including Liu'an, Shangrao, Xinyu and Huaihua. The dark blue anomaly of the mid-western cities in Figure 7B reveals COVID cases adjacent to industrial areas, and the light blue in the Midsouth shows a smaller industrial base and greater COVID risk. In the housing price layer, dark red represents low COVID risk areas in several areas with high house prices, whereas more blue areas represent a correlation between house prices and high COVID risk, with light blue covering almost the entirety of the central region. The impact of public green space and consumer sites layers is similar to that of house prices, with light blue in central and southern cities indicating communities further away from public green space and consumer sites exhibita greater COVID risk.

Timing characteristics of COVID risk based on the CIT index

In the 30 cities studied, there were 53,183 communities with 2,387 of them having cases of COVID-19, which accounts for 4.5%. In addition, the proportion of communities with house prices lower than the city average was found to be 70% (1,672/2,387). Taking "low community infrastructure levels in the community are not the cause of COVID-19" as H0, the null hypothesis was rejected in 80% of the cities (24/30). The weighted average odds ratio of the low community infrastructure levels

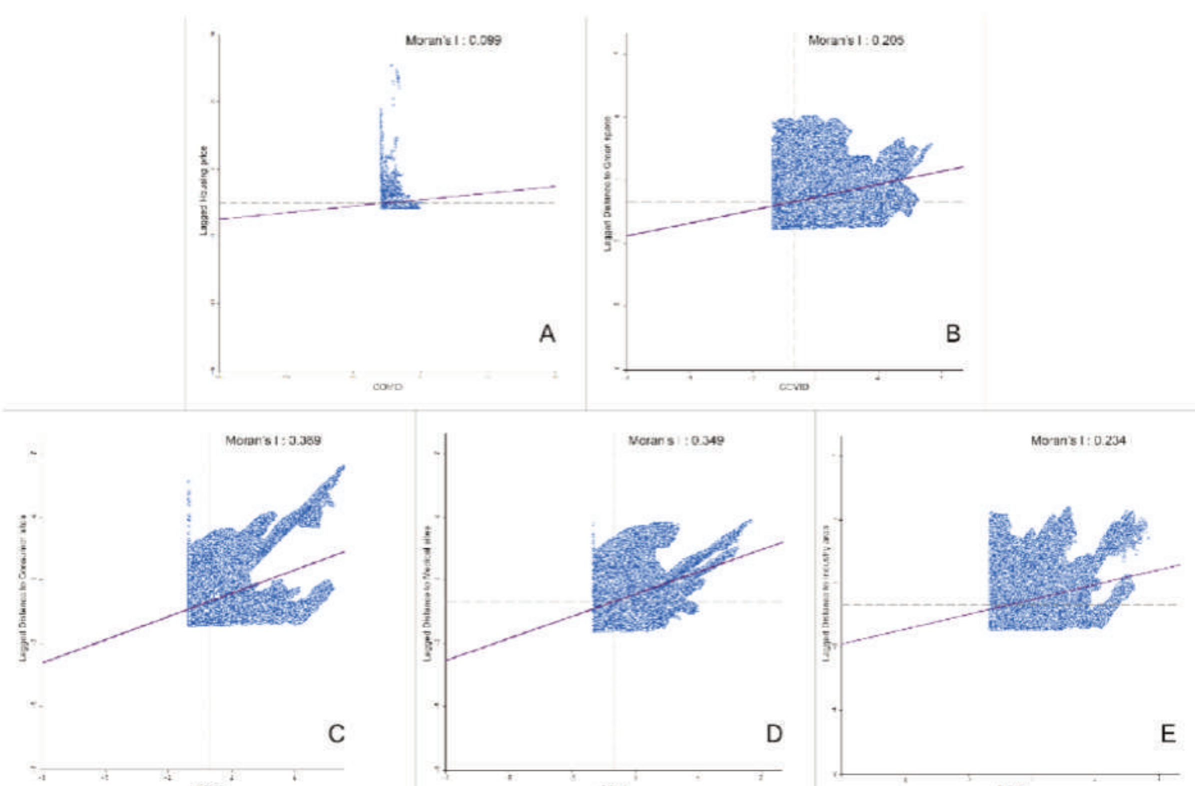

Figure 6. Global univariate bivariate Moran's I autocorrelation scatterplot of 5 layers. The fitted states in the subplots represent the spatial correlation of the 5 layers with COVID risk, and the x-coordinates of all subplots are COVID, and the y-coordinates indicate **A**) housing price, **B**) green space, **C**) consumer sites, **D**) medical sites, **E**) industy area, respectively.

in 30 cities reached 3.0 (95% CI), and the weighted average odds ratio of all cities where the null hypothesis was rejected was 3.035 (95% CI, Figure 8). The KDE curve allowed an intuitive comparison of the non-normally distributed COVID house price data and observation of the deviation of the curve over time (Figure 9).

Following the introduction of the per capita GDP indicator, the COVID-19 risk in low socioeconomic areas exhibited a more obvious trend (Figure 8). Cities with a per capita GDP of more than 100k have a weighted average COVID-19 risk of 1.69 in neighbourhoods with lower house prices. Cities with a per capita GDP of between 100k and 40k have a COVID-19 risk of 3.74 (95% CI), and cities with a per capita GDP that is lower than 40k have a weighted odds ratio of 4.62 (95% CI). These results suggest that house prices significantly impact COVID-19 risk, particularly in low-GDP cities. In addition, a negative correlation was found between the per capita GDP of all 30 cities and the odds ratio index in low-cost communities (r=-0.48, 95% CI).

Average house price has simply been used as a classifier for COVID. When the Receiver-Operating Characteristic (ROC)

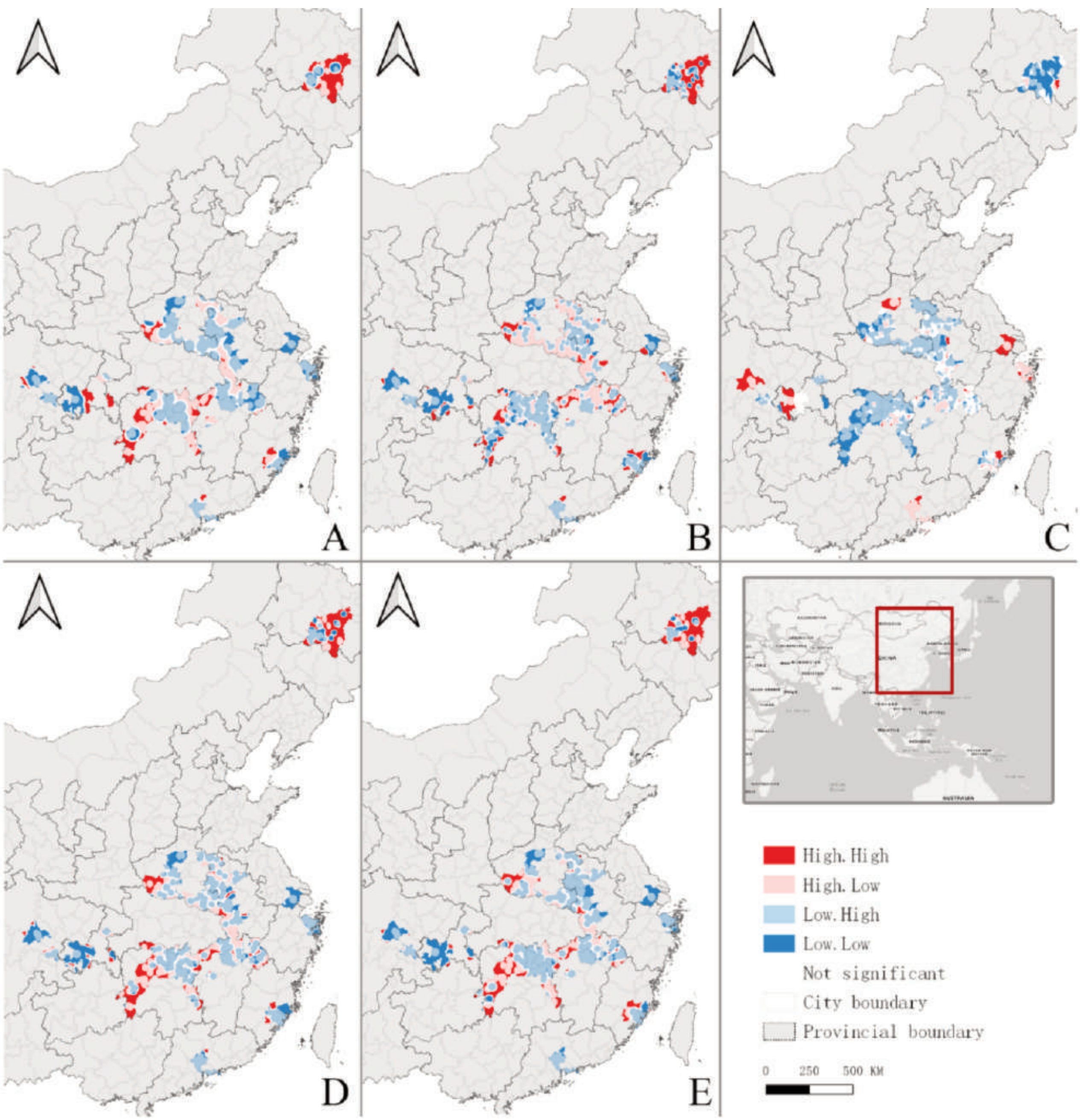

Figure 7. LISA map for spatial dependence between COVID-19 and community environmental factors. **A**) medical sites, **B**) industryareas, **C**) house prices, **D**) green-space, **E**) consumer sites.

curve for all 30 cities were standardized and drawn uniformly, the AUC was 0.58. When the ROC was conducted on 24,961 communities in 21 cities that had a per capita GDP of lower than 100k, the AUC increased to 0.63. When ROC curve was conducted for 10,405 communities in 10 cities that had a per capita GDP of below 40k, the AUC increased to 0.66 (Figure 10). It is generally effective to predict the risk of COVID with low house prices, particularly in cities that have a lower GDP (Figure 11).

Cities of China	NO. of COMM	COMM with Low house-price	COVID-19 High house-price	100M Yuan/10K People (GDP/Capita)	Odds Ratio(95% CI)	p Value
High-GDP/capita						
Suzhou	497	5	10	47.55	0.489 (0.165~1.454)	1.97E-01
Shenzhen	3939	92	90	20.67	1.024 (0.76~1.379)	8.79E-01
Guangzhou	9330	125	75	15.85	1.685 (1.262~2.251)	4.07E-04
Changsha	4219	88	52	13.49	1.724 (1.217~2.443)	2.32E-03
Ningbo	4124	45	47	13.1	0.956 (0.633~1.446)	8.35E-01
Chengdu	583	5	8	11.72	0.618 (0.2~1.913)	4.05E-01
Hefei	1900	69	23	11.64	3.165 (1.956~5.122)	1.62E-06
Quanzhou	2585	48	5	11.43	9.939 (3.943~25.05)	3.49E-09
Zhengzhou	1045	20	7	11.17	2.933 (1.229~6.999)	1.24E-02
Summary	**28222**	**497**	**317**		**1.690 (1.412~1.967)**	
Mid-GDP/capita						
Nanchang	2934	95	35	9.51	2.839 (1.913~4.214)	1.42E-07
Xinyu	498	77	12	9.39	9.751 (5.1~18.646)	4.74E-12
Chongqing	1184	81	21	7.98	4.36 (2.655~7.161)	2.83E-09
Zhuzhou	1171	53	15	6.54	3.81 (2.12~6.846)	3.92E-06
Yueyang	1074	65	21	6	3.413 (2.051~5.678)	2.09E-06
Changde	1121	46	12	5.82	4.11 (2.151~7.851)	7.76E-06
Harbin	3377	71	79	5.52	0.895 (0.644~1.242)	5.16E-01
Jiujiang	1318	46	14	5.51	3.466 (1.885~6.372)	3.61E-05
Pingdingshan	371	27	6	4.1	5.165 (2.073~12.868)	2.57E-04
Bengbu	870	59	34	4.07	1.872 (1.196~2.93)	9.19E-03
Yiyang	638	32	2	4	17.778 (4.22~74.886)	2.68E-07
Summary	**14556**	**652**	**251**		**3.740 (3.269~4.211)**	
Low-GDP/capita						
Anqing	1266	32	10	3.63	3.321 (1.618~6.818)	6.87E-04
Nanyang	1433	64	14	3.56	4.952 (2.749~8.921)	1.45E-08
Neijiang	815	22	7	3.43	3.27 (1.38~7.746)	5.35E-03
Shangqiu	1467	64	10	3.26	6.957 (3.542~13.666)	3.31E-10
Huaihua	600	24	6	3.04	4.276 (1.72~10.627)	1.02E-03
Xinyang	1481	142	32	2.7	5.401 (3.617~8.066)	6.87E-17
Shangrao	1271	51	6	2.63	9.188 (3.912~21.577)	2.52E-09
Bozhou	514	26	19	2.44	1.421 (0.763~2.645)	2.90E-01
Liu'an	544	32	3	2.07	12.108 (3.657~40.085)	8.95E-07
Fuyang	1014	66	40	1.64	1.761 (1.161~2.67)	1.16E-02
Summary	**10405**	**523**	**147**		**4.622 (4.202~5.042)**	
Summary	**53183**	**1672**	**715**		**3.035 (2.807~3.264)**	

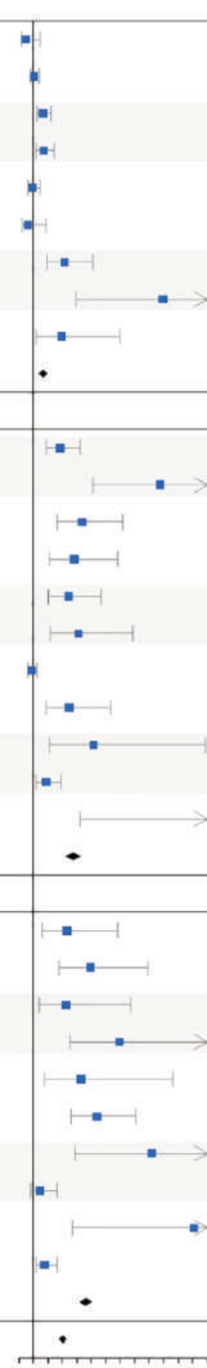

Figure 8. Forest map of COVID-19 risk in communities in 30 cities. This figure not only shows the COVID risk of low housing price neighbourhoods in various cities, but also shows that lower urban economic levels (GDP) tend to represent higher COVID risk.

Discussion

Containment and ultimate eradication of an infectious disease requires interdisciplinary collaboration as transmission and spread not only depend on the nature of the pathogen, but on various environmental factors and socioeconomic characteristics. A better understanding of all these factors and their interdependencies are essential for identifying the best strategies for containing the pathogen and protecting the population. The aim of this study was to examine the spread of the COVID-19 pandemic by analysing the community-scale relationships between communities with COVID-19 and the environmental indicators including medical sites, consumer sites, green space, industry sites, house prices community GDP.

A negative spatial dependency between communities with COVID-19 and house prices in a spatial perspective was found. Many cities in China were found to be defined as economically underdeveloped, with outflow sources of migrant workers. The positive correlation between house prices and environmental indices means that traditional urban centers have more medical sites, green spaces, industrial sites and consumption resources. However, the negative relationship between house prices and COVID-19 risk implies that some areas with low house prices have an unduly high risk of the disease. Interestingly, we found a positive spatial dependency between communities with COVID-19 and green space. The initial hypothesis was that industry may cause additional pollution, leading to an increased risk of COVID-19 infection, while public green space acts as a ventilation and exercise areas reduc this risk. However, the regional correlations found in the data appeared to be different from this hypothesis and exhibit no stable abnormal pattern, something that may be due to the fact that there was no differentiation between industrial types. Different pollutants and pollution patterns, even rivers, topography and wind direction can all affect pollution severity, with the health-promoting effect of public green space not appearing to be enough to provide an advantage regarding COVID risk. It should, however, be noted that the COVID-19 risk (as treated in this study) refers to the risk of new infections. Even though this study results suggest that the population and the degree of aging of cities do not have a statistically significant contributions to the new such infections, it does not mean that the elderly and those living in densely populated areas can ignore the long-term health impacts of COVID-19, especially in the context where long COVID has been increasingly verified.

The use of spatial and temporal monitoring methods enabled the study of the impact of community settings on COVID-19 risk. International studies have shown that the population distribution and economic conditions of different cities can be used to determine the infection and transmission rates. Residents who live in low-cost communities have a greater likelihood of facing economic distress and cannot obtain adequate medical services or maintain social distancing (Ahmad *et al.*, 2020; Sharma & Yount, 2020). The findings of this study show that house prices have a significant correlation with COVID-19 risk, which is consistent with the conclusions of many other studies, such as those by Lau *et al.* (2020) and Wasdani and Prasad (2020). Many studies have reported simi-

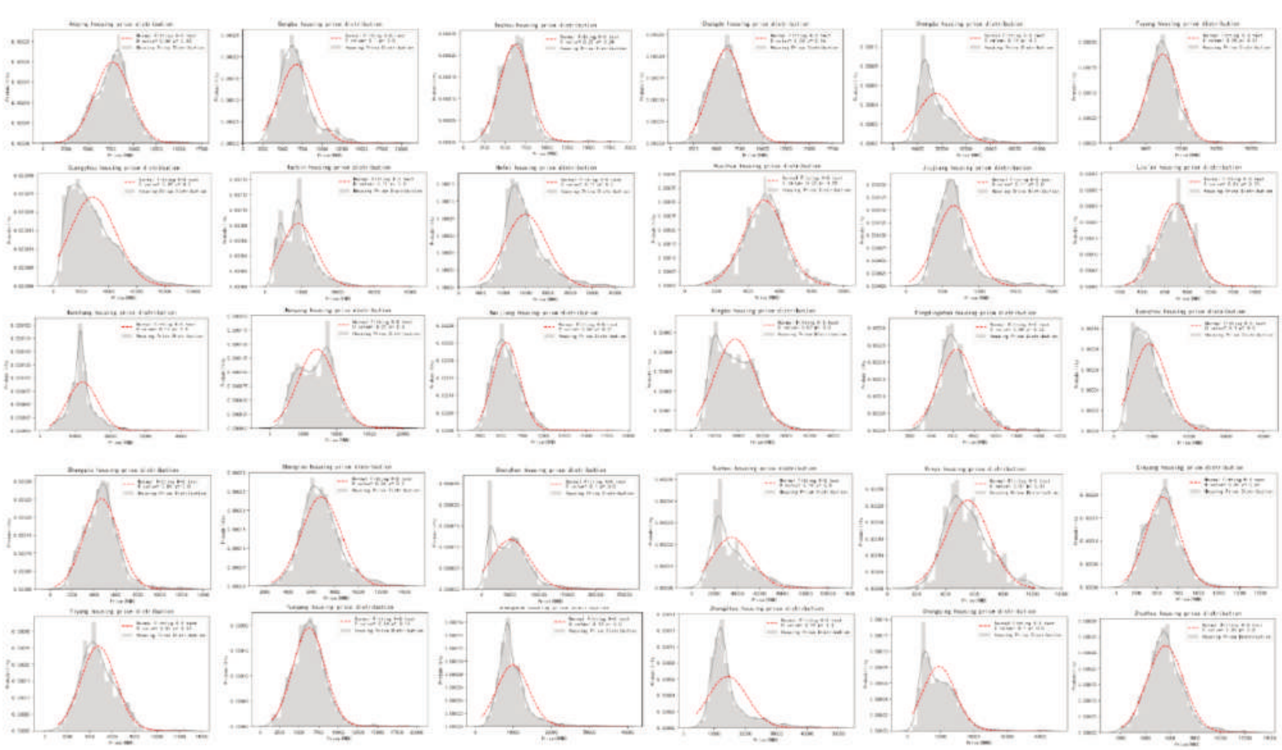

Figure 9. Housing price-frequency distribution and normal test in 30 cities. The x-coordinates of all subplots are prices and the y-coordinates are frequencies. The gray histogram represents the distribution of housing prices in each city, and the red dotted line represents the results of the K-S test.

lar results from low-socioeconomic environmental studies of other vector-borne and infectious diseases, *e.g.*, malaria, tuberculosis and H1N1 influenza (Balogun *et al.*, 2019; Dawaki *et al.*, 2016; Ghani *et al.*, 2019; Rukmanee *et al.,* 2014). A strong positive correlation can often be found between literacy level, income, and house prices in residential areas ((Coker *et al.*, 2011); Dowd *et al.*, 2020), and the average life expectancy of low-socioeconomic groups such as black people during the pandemic is much lower than that of other races (Bong *et al.*, 2020; Millett, 2020). This appears to be consistent with the understanding of this research. House prices were found to have no apparent strong correlation with MCGIs, as is generally believed by other researchers (Rocha *et al*.,2021). Prior to this study, house prices were proven to be correlated with the income of residents, their living habits, environmental pollution, chronic diseases, and occupations (A and B), all of which can impact COVID-19 risk. Further research on house price and COVID-19 risk differences is required.

This study demonstrates that a spatial link between community environment and COVID-19 risk, particularly community infrastructure represented by house prices, can be used as a proxy for the evaluation of this risk in low socioeconomic groups. This is of great significance to the health equality of low-socioeconomic

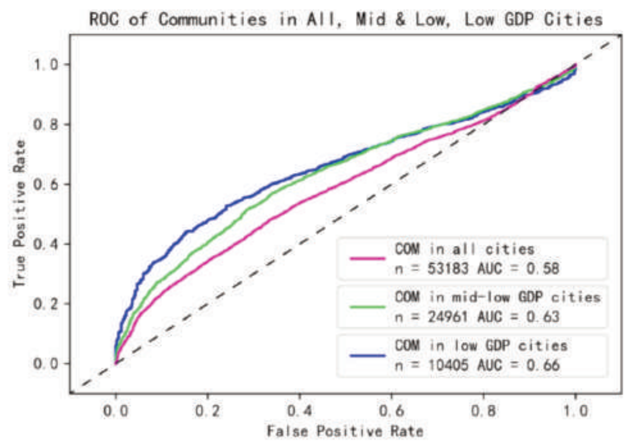

Figure 10. Receiver-operating characteristic (ROC) of classifier by average house price in all, mid-low, and low GDP city communities. The housing price classifier visually shows the city's economic situation and the trend of low-price neighbourhood risk: In cities with lower economic levels, the housing price classifier can better screen out neighbourhoods with high COVID risk.

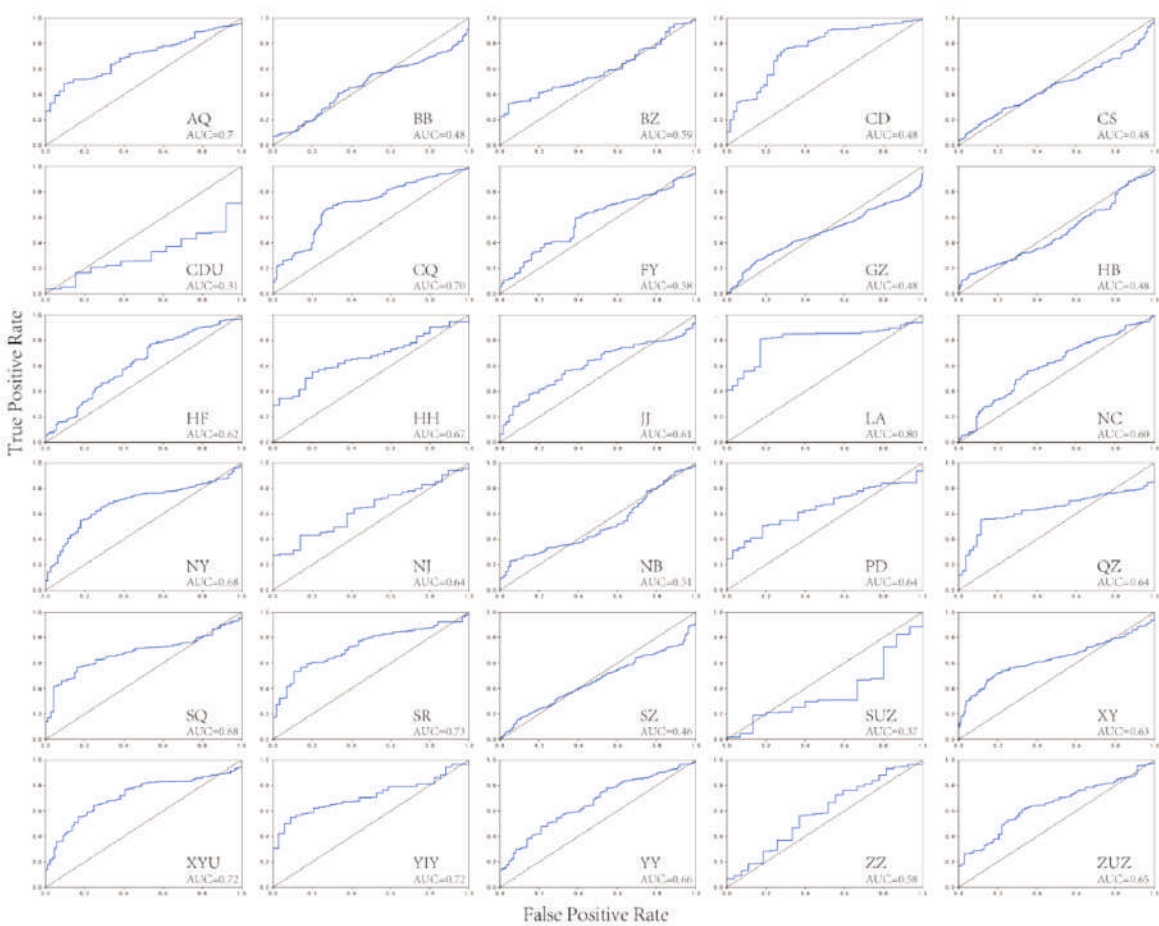

Figure 11. Receiver-operating characteristic (ROC) of classifier by average house price in 30 cities. AQ, Anqing, BB, Bengbu, BZ, Bozhou, CD, Changde, CS, Changsha, CDU, Chengdu, CQ, Chongqing, FY, Fuyang, GZ, Guangzhou, HB, Harbin, HF, Hefei, HH, Huaihua, JJ, Jiujiang, LA, Lu’an, NC, Nanchang, NY, Nanyang, NJ, Neijiang, NB, Ningbo, PD, Pingdingshan, QZ, Quanzhou, SQ, Shangqiu, SR, Shangrao, SZ, Shenzhen, SUZ, Suzhou, XY, Xinyang, XYU, Xinyu, YIY, Yiyang, YY, Yueyang, ZZ, Zhengzhou, ZUZ, Zhuzhou.

groups in developing countries. The inequality of social resources that are hidden behind the inequality of COVID-19 risks requires greater attention.

Conclusions

By examining the interplay between COVID-19 and communityenvironmentbased on a gridscale, this study can be used to help mitigate the rate of spreading and the severity of the disease, while also advocating for greater attention to areas with a higher risk of infection. Our analysis demonstrates that, even under the circumstances where the sample size for diseases is 2,387 and that for housing prices is 55,570, housing prices have a highly significant positive correlation with COVID-19, which implies that housing prices are relatively lower in the vicinity of a COVID-19 community.In addition, significant low-low and high-high clusters of COVID-19 cases and deaths and diabetes were found in the Midwest and the South, area colloquially known as the "stroke belt" where there is a significantly higher stroke rate than in the rest of the country. Interestingly, no significant spatial correlation was found between COVID-19 cases and deaths and the number of primary care providers (PCPs), prevalence of adult obesity and diabetes, number of uninsured individuals, or flu vaccination. Finally, this study confirms previous findings that poor people have an increased risk of infection. In particular, a positive significant spatial dependence between house price and COVID-19 cases was found, which can possibly be explained by poor living standards, insufficient access to healthcare facilities, and living in areas where there is higher population density.

References

Ahmad K, Erqou S, Shah N, Nazir U, Morrison AR, Choudhary G, Wu WC, 2020. Association of poor housing conditions with COVID-19 incidence and mortality across US counties. PLoS One 2020;15:e0241327.

Balogun MR, Sekoni AO, Meloni ST, Odukoya OO, Onajole AT, Longe-Peters OA, Ogunsola FT, Kanki PJ, 2019. Predictors of tuberculosis knowledge, attitudes and practices in urban slums in Nigeria: A cross-sectional study. Pan Afr Med J 32:14622.

Barmby T, Larguem M, 2009. Coughs and sneezes spread diseases: An empirical study of absenteeism and infectious illness. J Health Econ 28:1012-1017.

Bong CL, Brasher C, Chikumba E, Mcdougall R, Enright A, 2020. The COVID-19 Pandemic: Effects on Low and Middle-Income Countries. AnesthAnalg 131:1.

Buikema AR, Buzinec P, Paudel ML, Andrade K, Johnson JC, Edmonds YM, Jhamb SK, Chastek B, Raja H, Cao F, Hulbert EM, Korrer S, Mazumder D, Seare J, Solow BK, Currie UM, 2021. Racial and ethnic disparity in clinical outcomes among patients with confirmed COVID-19 infection in a large US electronic health record database. EClinicalMedicine 39:101075.

Cellmer R, 2011. Spatial analysis of the effect of noise on the prices and value of residential real estates. Inf Tec Econ Ag 110:400-13.

Coker RJ, Hunter BM, Rudge JW, Liverani M, Hanvoravongchai P, 2011. Emerging infectious diseases in southeast Asia: regional challenges to control. Lancet 377:599-609.

Cordes J, Castro MC, 2020. Spatial analysis of COVID-19 clusters and contextual factors in New York City. Spat Spatiotemporal Epidemiol 34:100355.

Crosby H, Damoulas T, Caton A, Davis P, Albuquerque JPD, Jarvis SA, 2018. Road distance and travel time for an improved house price Kriging predictor. Geo-spat Inf Sci 21:185-94

Cuong HQ, Vu NT, Cazelles B, Boni MF, Anders KL, 2013. Spatiotemporal Dynamics of Dengue Epidemics, Southern Vietnam. Emerg Infect Dis 19:945-53

Dawaki S, Al-Mekhlafi HM, Ithoi I, Ibrahim J, Atroosh WM, Abdulsalam AM, Sady H, Elyana FN, Adamu AU, Yelwa SI, 2016. Is Nigeria winning the battle against malaria? Prevalence, risk factors and KAP assessment among Hausa communities in Kano State. Malar J 15:351.

DHS, 2020. The Demographic and Health Surveys (DHS) Program. 2020. Available from: https://dhsprogram.com/

Dowd JB, Andriano L, Brazel DM, Rotondi V, Mills MC, 2020. Demographic science aids in understanding the spread and fatality rates of COVID-19. Proc Natl Acad Sci USA 117:202004911.

Finch WH, Hernández Finch ME. Poverty and Covid-19: Rates of Incidence and Deaths in the United States During the First 10 Weeks of the Pandemic. Front Sociol 2020;5:47.

Ghani, Nurul, Akmar, Shohaimi, Shamarina, Hee, Alvin, Kah-Wei, Chee, Hui-Yee, 2019. Comparison of knowledge, attitude, and practice among communities living in hotspot and non-hotspot areas of dengue in Selangor, Malaysia. Trop Med Infect Dis 4(:37.

Hansen C, Edwards, Scalia G, Tomba, Freiesleben B, Blasio D, 2016. Influenza in workplaces: transmission, workers' adherence to sick leave advice and European sick leave recommendations. Eur J Public Health 26:478-85.

Hopkins J, 2020. The Johns Hopkins Coronavirus Resource Center. 2020. Available from: https://coronavirus.jhu.edu/

Jim C, Chen W, 2006. Impacts of urban environmental elements on residential housing prices in Guangzhou (China). Landscape Urban Plan 78:422-34.

Lantz PM, House JS, Lepkowski JM, Williams DR, Chen J, 1998. Socioeconomic Factors, Health Behaviors, and MortalityResultsFrom a Nationally Representative Prospective Study of US Adults. J Am Med Assoc (JAMA) 279:1703-08.

Lau LL, Hung N, Go DJ, Ferma J, Wei X, 2020. Knowledge, attitudes and practices of COVID-19 among income-poor households in the Philippines: A cross-sectional study. J Glob Health 10:011007.

Millett GA, Jones AT, Benkeser D, Baral S, Mercer L, Beyrer C, Honermann B, Lankiewicz E, Mena L, Crowley JS, Sherwood J, Sullivan PS, 2020. Assessing differential impacts of COVID-19 on black communities. Ann Epidemiol 47:37-44.

Pak A, Adegboye OA, Adekunle AI, Rahman KM, Eisen DP, 2020. Economic Consequences of the COVID-19 Outbreak: the Need for Epidemic Preparedness. Front Public Health 8:1-4.

Pant S, Yadav EN, Sharma M, Bedi Y, Raturi A, 2024. Web Scraping Using Beautiful Soup. in Proceedings 2024 International Conference on Knowledge Engineering and Communication Systems (ICKECS) 2024. 1. IEEE Xplore. doi: 10.1109/ickecs61492.2024.10617017

Pearson C, 2015. The future of life expectancy and life expectancy inequalities in England and Wales: Bayesian spatiotemporal forecasting. Lancet 2015;386:163-70.

Pettinicchio D, Maroto ML, Chai L, Lukk M, 2021. Findings from an online survey on the mental health effects of COVID-19 on Canadians with disabilities and chronic health conditions. Disabil Health J 14:101085.

Platform, The National Health Commission of the People's Republic of China and Alibaba UC Intelligent Information Service. 2020. COVID-19 community tracker, Accessed 20 Mar. Available from: https://pages.uc.cn/r/feiyan-map/FyMapPageMap.

Price-Haywood EG, Burton J, Fort D, Seoane L, 2020. Hospitalization and Mortality among Black Patients and White Patients with Covid-19. N Engl J Med 382:2534-43.

Qian X, Qiu S, Zhang G, 2021. The impact of COVID-19 on housing price: Evidence from China. Financ Res Lett 43:101944.

Rocha R, Atun R, Massuda A, Rache B, Spinola P, Nunes L, Lago M, Castro MC, 2021. Effect of socioeconomic inequalities and vulnerabilities on health-system preparedness and response to COVID-19 in Brazil: a comprehensive analysis. Lancet Glob Health 9:e782-e792.

Rukmanee N, Yimsamran S, Rukmanee P, Thanyavanich N, Pan-Ngum W, 2014. Knowledge, attitudes and practices (kap) regarding influenza A (H1N1) among a population living along Thai-Myanmar border, Ratchaburi Province, Thailand. Southeast Asian J Trop Med Public Health 45:825-33.

Sharma K, Yount KM, 2020. Burdening the poor: Extreme responses to COVID-19 in India and the Southeastern United States. J Glob Health 10:020327.

Skatun JD, 2003. Take some days off, why don't you?: Endogenous sick leave and pay. J Health Econ 22:379-402.

Sousa ARD, Teixeira JRB, Moreira WC, Santos MB, Carvalho HEFd, Almeida RS, Florencio RMS, Queiroz AMd, Merces MCD, Mota TN, 2022. Psychological Distress in Men During the COVID-19 Pandemic in Brazil: The Role of the Sociodemographic Variables, Uncertainty and Social Support. Int J Environ Res Public Health 19:350.

Tobler WR, 1970. A computer movie simulating urban growth in the Detroit region. Econ Geogr 46:234-240.

van den Broek-Altenburg EM, Atherly AJ, Diehl SA, Gleason KM, Hart VC, MacLean CD, Barkhuff DA, Levine MA, Carney JK, 2021. Jobs, Housing and Mask-Wearing: A Cross-Sectional Study of Risk Factors for COVID-19. JMIR Public Health Surveill 7:e24320.

Wasdani KP, Prasad A, 2020. The impossibility of social distancing among the urban poor: the case of an Indian slum in the times of COVID-19. Local Environ 25:414-8.

Woo B, Jun J, 2022. COVID-19 Racial discrimination and depressive symptoms among Asians Americans: does communication about the incident matter? J Immigr Minor Health 24:78-85.

Yang TC, Kim S, Zhao Y, Choi SWE, 2021. Examining spatial inequality in COVID-19 positivity rates across New York City ZIP codes. Health Place 69:102574.

Zheleznyak EV, Khripach LV, 2014. The use of open real estate databases for the analysis of influence of concomitant factors on the state of the urban population's health. Gig Sanit 94: 92-4.